Proposal of a Methodology for Evaluating Photovoltaic Inverter Performance Using a Novel Performance Ratio

Andrei da Cunha Lima[1], Charles Schardong[1], Ricardo Bortolini[1], Frederico Schaf[1], Cassiano Rech[1], Lucas Bellinaso[1], Leandro Michels[1]

[1] *Federal University of Santa Maria, Santa Maria (Brazil)*

Abstract

This paper presents the development of a methodology to evaluate and compare inverters under various operating conditions. In photovoltaic power plants, inverter efficiency depends on both electrical and thermal operating points. Due to fluctuations caused by several factors in real-world photovoltaic installations, comparing different inverters can be challenging. To address this, a test setup was developed to apply the same electrical and thermal conditions to different inverters, enabling fair comparisons under identical scenarios. As a result, a new performance ratio is proposed, based on experimental data obtained from three inverters with the same output power level. The test results also enhanced energy yield estimation by accounting for thermal effects, which revealed significant performance differences among the three inverters.

Keywords: Methodology, Operating conditions, Setup, Efficiency, Performance Ratio

1. Introduction

In recent decades, photovoltaic (PV) solar energy has emerged as a key technology in the global transition toward sustainable power systems. Its widespread adoption has been driven by continuous technological improvements, significant cost reductions, and growing environmental awareness regarding renewable energy sources. In Brazil, this global trend is reflected in a remarkable increase in installed PV capacity, encompassing both distributed generation (DG) and centralized generation (CG) systems. This expansion has been further reinforced by the enactment of Law No. 14,300/2022 — the *Legal Framework for Distributed Generation* — which established a comprehensive regulatory foundation to foster the sustainable development of the national photovoltaic sector.

According to data from the Brazilian Photovoltaic Solar Energy Association (ABSOLAR, 2025), Brazil surpassed 55 GW of installed photovoltaic (PV) capacity by July 2025, with more than 60% of this capacity connected through distributed generation (DG) systems. This significant expansion is attributed not only to the country's favorable solar irradiance conditions—exceeding 5 kWh/m² across most of its territory—but also to public incentive policies, dedicated financial mechanisms, rising electricity tariffs, and increased environmental awareness (EPE, 2023; ANEEL, 2023). Given the rapid growth of PV deployment in the Brazilian energy mix, the development of more accurate and standardized approaches for assessing the performance of photovoltaic inverters has become essential, as these devices play a critical role in energy conversion and overall system efficiency.

However, the efficiency models currently employed do not adequately account for the impact of thermal dynamics throughout the day on the energy conversion efficiency of photovoltaic inverters, particularly under conditions of thermal derating and DC oversizing (Lima et al., 2023). Well-established testing protocols, such as the one proposed by Sandia National Laboratories, define specifications and requirements for evaluating the performance of grid-tied photovoltaic inverters. Nevertheless, the thermal conditions specified in these standardized tests do not accurately represent the real operating environments found in tropical and subtropical regions, such as Brazil, where wide climatic variability poses additional challenges for assessing and modeling inverter performance under real-world conditions.

In this context, the present work proposes a new methodology for inverter performance analysis, aiming to enhance experimental characterization and enable fair comparison among different technologies under real operating conditions. To address these limitations, this study proposes an experimental methodology for evaluating the performance of photovoltaic inverters under dynamic operating conditions throughout a typical solar day. The proposed approach simulates the inverter's thermal and electrical behavior considering a 120% DC oversizing of the photovoltaic array, while ambient temperature is controlled using a thermal chamber. This methodology enables a

10.18086/swc.2025.03.60 Available at http://proceedings.ises.org

quantitative assessment of the influence of thermal variations and real operating conditions on the actual energy converted over the course of the day. Consequently, it provides a more representative experimental framework for Brazilian conditions, contributing to the refinement of inverter efficiency models and supporting fair comparisons among different inverter technologies.

2. Methodology for inverter performance evaluation

The methodology used to evaluation the performance of PV inverters is based on the following assumptions:

- The maximum peak power of the PV array is oversized in relation to rated power of the PV inverter (often exceeding than 120%);
- PV inverters topologies have two conversion stages, enabling multiple independent MPPT inputs;
- PV inverters inputs have a wider operational voltage range and impose a current limit;
- PV inverters are typically designed without external fans and with a small heatsink area, resulting in a significant impact of the temperature on their performance.

As a result, static efficiency approaches outlined in standards such as IEC 62891 (IEC, 2019), EN 50530 (EN, 50530), and the Sandia Inverter Performance Test Protocol Efficiency are not the most suitable for evaluating the performance of PV inverters. A more appropriate approach involves calculating a performance ratio that compares the average annual energy production of the inverter in comparison of an ideal inverter, as defined by:

$$PR_{inv}(\%DC_{or}, \%Vdc_{nom}, \%iDc_{max}) = \frac{E_{inv}}{E_{ideal,inv}} \quad \textit{(eq. 1)}$$

Where:

- PR_{inv} is the inverter performance ratio under a given test condition.
- $\%Dc_{or}$ represents the percentage of DC input power oversizing of the photovoltaic inverter relative to its nominal rating, given by Equation 2.
- $\%vdc_{nom}$ is the ratio between the maximum power point (MPP) voltage of the photovoltaic string under standard test conditions (STC) and the nominal DC input voltage v_{DCnom}, considering identical strings connected to each inverter input.
- $\%IDc_{max}$ denotes the ratio between the maximum current of the photovoltaic string under STC and the maximum DC input current i_{DCmax} of the inverter, also assuming identical strings at all inputs.
- $E_{ideal,inv}$ corresponds to the energy that would be produced by an ideal inverter with nominal power P_{nom}, expressed in kilowatt-hours (kWh).
- Finally, E_{inv} represents the output energy of the inverter under test, whose nominal power is defined as P_{nom}, also expressed in kilowatt-hours (kWh).

$$\%DC_{or} = \frac{P_{nom}}{Pdc_{pk}} \quad \textit{(eq. 2)}$$

Where:

- P_{nom} if the nominal power of Inverter Under Test (IUT).
- Pdc_{pk} is the peak power of photovoltaic string.

The testing procedure aims to evaluate the performance of photovoltaic (PV) inverters by emulating, in a controlled laboratory environment, operating conditions similar to those encountered in real-world applications.

In order to create a test protocol compatible with Brazilian scenarios and emulate similar conditions found in applications, a methodology based on 8 steps was developed that can be applied to both small inverters (usually used in DG) and large inverters (used in GC plants).

The steps of the proposed methodology are described below.

- **Step 1:** Define the reference photovoltaic system design suitable for the IUT, considering the installation site, array orientation and tilt angle, mounting structure, module technology, and the DC oversizing factor.
- **Step 2:** Obtain the solar irradiance data on the plane of array (GPOA) and the ambient temperature (Tamb) corresponding to the site defined in Step 1, using meteorological information systems or other reliable data sources.
- **Step 3:** Select a representative typical day that characterizes critical operating conditions for the inverter, determining the corresponding irradiance and temperature profiles to reproduce scenarios of higher thermal and electrical stress for the photovoltaic system. The diurnal soil and air temperature variation was based on Parton and Logan (1981).
- **Step 4:** Generate one-minute-resolution I–V curves representing the electrical characteristics of the PV arrays defined in Step 1, based on the irradiance and temperature conditions established in Step 3. To obtain POA irradiance, was considered the model of Perez. (Perez *et al.*, 1987). The array performance estimation followed the approach proposed by Kratochvil et al. (2004) and further validated by Soto et al. (2006).
- **Step 5:** Install the photovoltaic inverter inside the environmental test chamber illustrated in Figure 3, attaching thermocouples or thermistors to the main internal components for continuous thermal monitoring during the experiment.
- **Step 6:** Initialize the climatic chamber and adjust its temperature to match the ambient temperature at sunrise for the typical day defined in Step 3. Continuously monitor the thermal sensors until all reach the target temperature set within the chamber.
- **Step 7:** Power on the AC grid simulator, configuring it to nominal frequency and voltage, and activate the DC source simulators (SAS) to reproduce the I–V curves defined in Step 4. Update, every minute, the SAS output parameters and the chamber temperature reference through a Python script. Continuously record the inverter's input and output power, energy, voltage, and current, as well as the temperatures measured by the thermocouples.
- **Step 8:** Perform post-processing of the recorded data to compute the inverter performance index, correlating the converted energy with the imposed environmental and electrical conditions throughout the test.

The steps of proposed methodology can be observed in Figure 1.

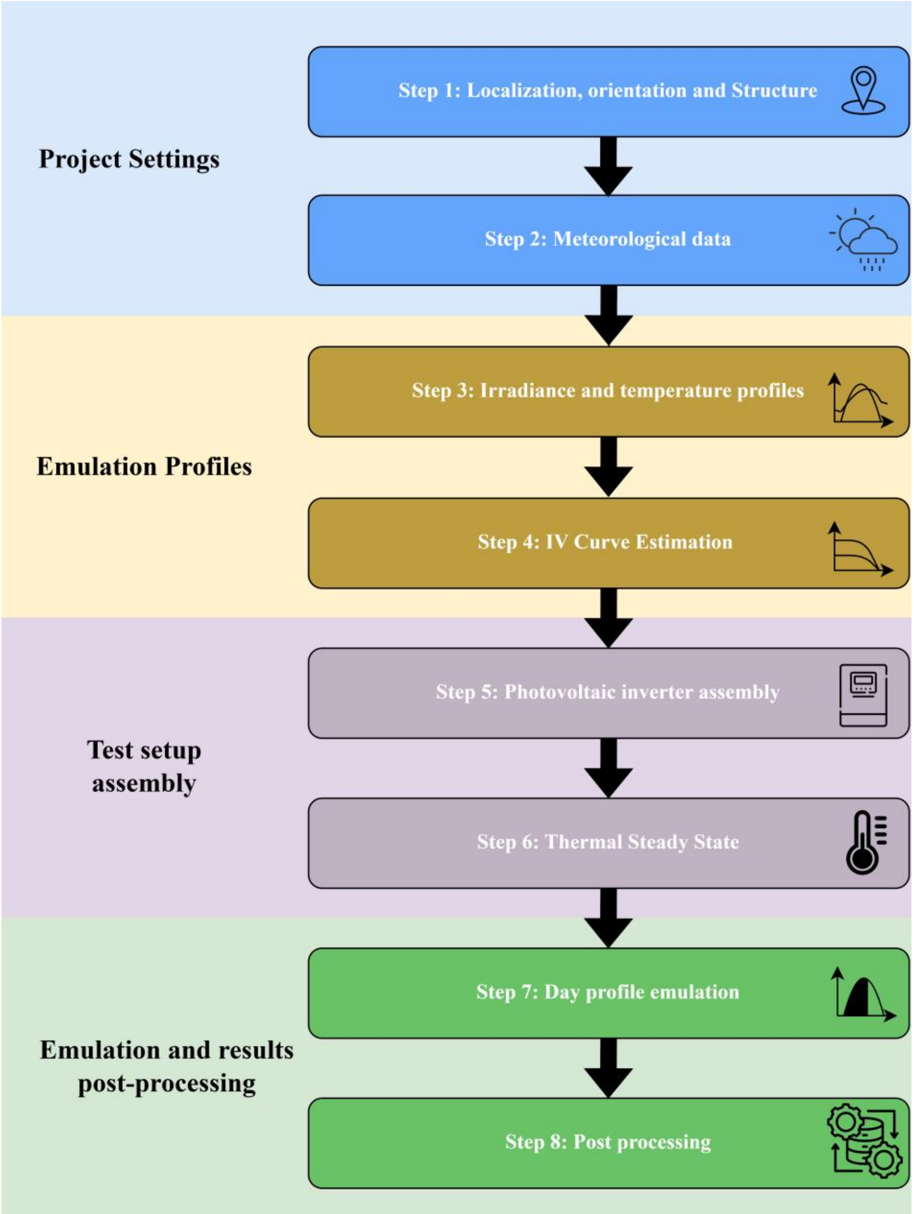

Figure 1: Methodology steps.

To implement the proposed methodology, a means of controlling the ambient temperature was required. Therefore, a thermal chamber was developed with the purpose of placing the IUT inside it and accurately emulating thermal conditions.

Within the chamber, the inverter is supplied through MPPT inputs controlled by photovoltaic array simulators (SAS), while its output is connected to a grid emulator. The entire test procedure is managed by a Python-based server, which monitors the measured quantities via a CAN bus and sends the corresponding control commands to the sources.

Data acquisition was performed using a GEN4tb measurement system operating at a sampling rate of 50 kSamples/s. Figure 2 presents a block diagram showing system behavior.

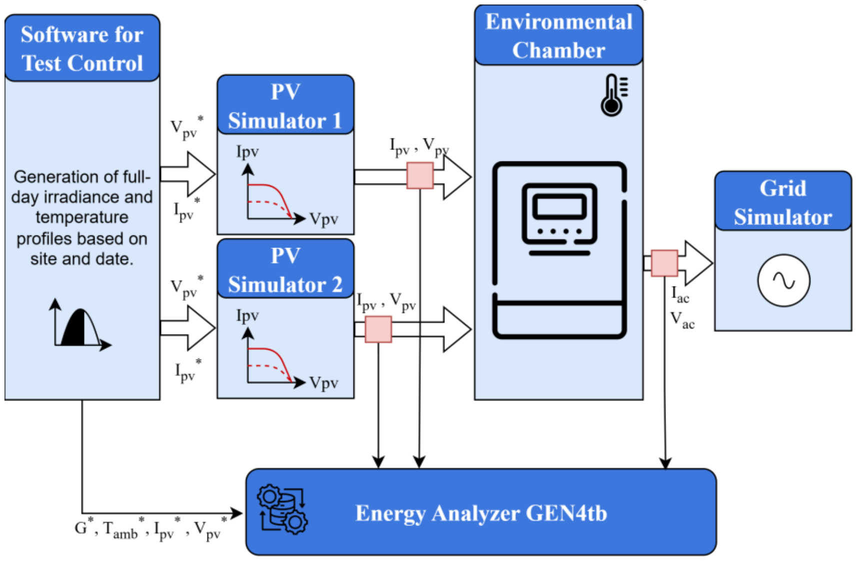

Figure 2: Block Diagram for test setup.

According to Figure 2, the proposed setup is composed of 5 main blocks: software for test control, PV simulator power sources, measurement instrument, test chamber and grid simulator.

The control software was developed to compute the profiles to be emulated by the power sources and to send thermal reference signals to the climatic chamber. Based on the selected location, the software accesses an external database to retrieve the meteorological data corresponding to the specified day and site. Using the local irradiance data, a transposition algorithm is applied to determine the effective irradiance incident on the photovoltaic array. Considering the installation type, azimuth, and tilt angle of the string, the effective irradiance on the array surface is accurately calculated.

Using the characteristics of the photovoltaic module model and the ambient temperature data, the software generates the I–V curve of the array, which is emulated by the photovoltaic source simulators with a one-minute time step. As output, the software produces a complete set of I–V profiles, enabling the emulation of an entire day of solar irradiance.

Communication with photovoltaic source simulators, the AC grid emulator, the power analyzer, and the climatic chamber is established via a CAN bus and Ethernet network, ensuring synchronized and automated test operation.

The photovoltaic source simulators are employed to reproduce the I–V curve at each point of the daily emulation. Through an Ethernet communication interface, up to 1024 voltage points and 1024 current points are transmitted to the source emulator, which is responsible for accurately reproducing the instantaneous operating conditions of the day.

The measurement equipment records the input and output voltages and currents of the IUT. In addition to electrical quantities, it also performs internal and external thermal measurements to monitor the thermal dynamics of the inverter's main components throughout the test. Finally, the reference signals used during the experiment are transmitted via the CAN bus from the control software to the power analyzer, ensuring that the test procedure can be accurately reproduced across different inverters.

The climatic test chamber was designed to emulate the thermal profile of a full simulation day, maintaining the IUT at a reference temperature defined by the control software. Through CAN communication, the control software sends a thermal reference to the chamber every minute, allowing it to regulate and maintain the DUT under the specified thermal conditions until the next temperature setpoint is received.

Finally, the grid emulator provides an electrical network interface for the IUT. Similar to the photovoltaic source simulators, the grid emulator receives the RMS voltage and frequency references from the control software via Ethernet. In this methodology, both the grid voltage and frequency are maintained at the nominal operating values specified for the equipment. Figure 3 presents the test setup used to reproduce the proposed methodology.

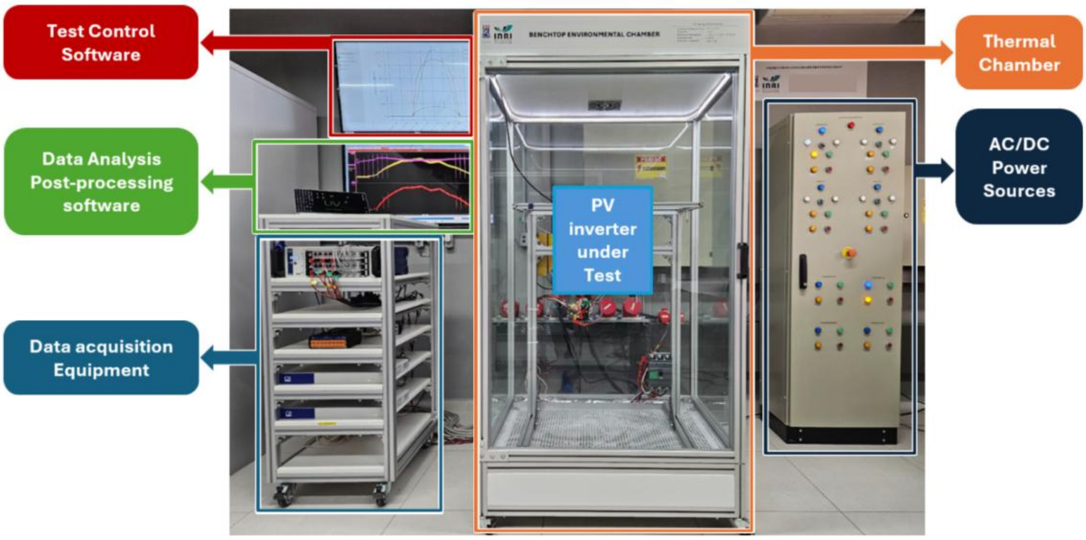

Figure 3: Experimental setup including control software, data acquisition system, thermal chamber, and power simulators.

As shown in Figure 3, the test control software (highlighted in red) is responsible for generating the daily profiles to be emulated during the experiment. The post-processing and data analysis software, indicated in green, manages all measurement acquisition and data storage throughout the test.

The power analyzer, marked in blue, performs electrical measurements at 50 kSamples/s. At the center of the figure, the thermal chamber houses the Inverter Under Test, while on the right side, the control panel of the DC source simulators (SAS) and AC grid emulator is displayed, both responsible for reproducing the profiles during the test.

To assess the thermal behavior of the device throughout the simulated day, the proposed methodology also includes the measurement of key thermal variables from the main internal components of the IUT. Figure 4 illustrates the mounting locations of all thermistors installed inside the equipment.

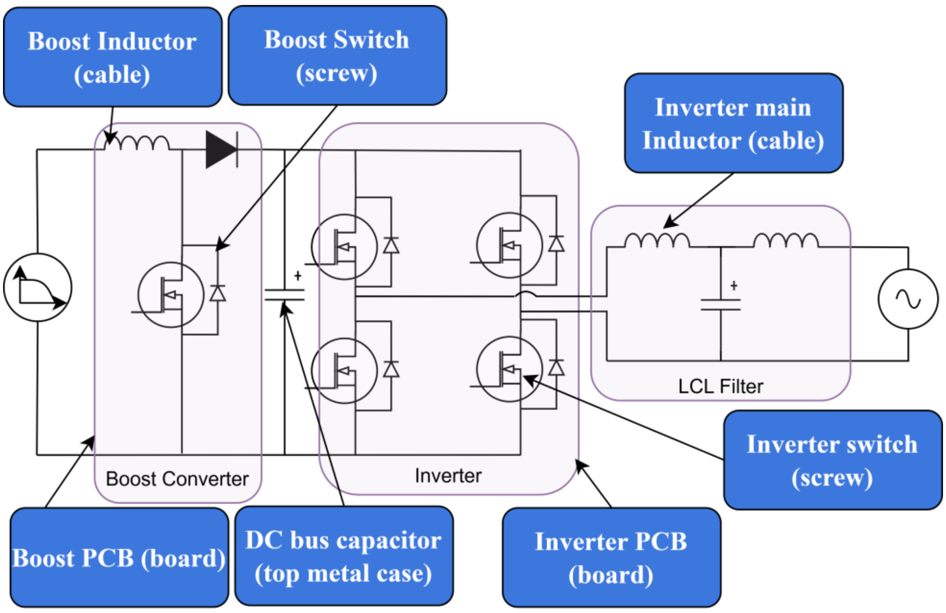

Figure 4: Mounting locations of thermistors used for monitoring the internal temperature of the IUT.

As shown in Figure 4, the thermistors were strategically installed on key components of the photovoltaic inverter to monitor the internal temperature distribution during operation. In the boost converter stage, sensors were mounted on the boost inductor (cable), the boost switch (screw), and the boost PCB (board).

At the DC link, one thermistor was placed on the DC bus capacitor, fixed to its top metallic case to capture thermal variations associated with energy storage and ripple current effects.

In the inverter stage, thermistors were positioned on the inverter main inductor (cable), the inverter switch (screw), and the inverter PCB (board). These measurement points enable the evaluation of thermal gradients across the main power conversion elements, providing insights into heat distribution and dynamic thermal response under realistic operating conditions.

3. Results and comparisons

The experimental tests were conducted based on a reference photovoltaic (PV) system located in Petrolina, Brazil (Latitude 9° 23′ 34″ S, Longitude 40° 30′ 28″ W). The PV array was oriented to the North, mounted on a fixed support structure with a tilt angle of 9°. Each string consisted of seven JAM72330-530/MR modules connected in series, resulting in a DC oversizing ratio of approximately 36% relative to the inverter nominal power.

Table 1 summarizes the electrical characteristics of the PV strings associated with each IUT. These parameters, defined under Standard Test Conditions (STC), were used as the basis for calculating the I–V profiles emulated during the experimental procedures.

Table 1: Electrical characteristics of PV strings.

	Inverter A	Inverter B	Inverter C
Per string			
STC Power (W)	3404	3404	3404
STC Voc (V)	345,1	345,1	345,1
STC Vmpp (V)	276,1	276,1	276,1
STC Isc (A)	13,7	13,7	13,7
STC Impp (A)	12,3	12,3	12,3
-Isc (per oC)	0,045 %	0,045 %	0,045 %
-Voc (per oC)	-0,275%	-0,275%	-0,275%
Total			
STC Power (W)	6809	6809	6809

Based on the parameters described above, an experimental test was carried out over a 12-hour period, during which 720 data points of irradiance and ambient temperature were acquired. The output power profiles of the IUT, obtained throughout the entire evaluation period, are presented in Figure 5.

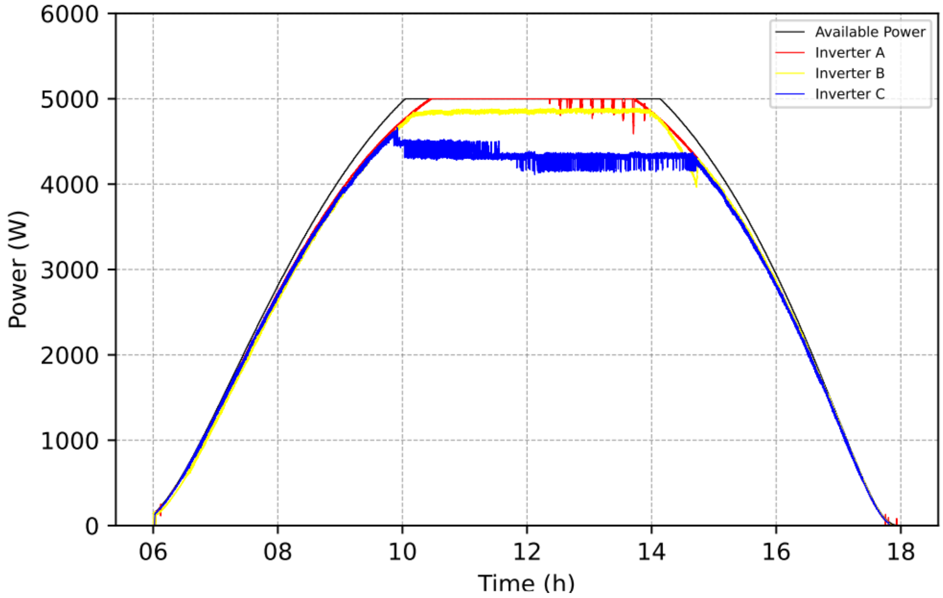

Figure 5: Output Power comparison between inverters considering same test procedure.

As shown in Figure 5, the output power of each device is presented. The black curve represents the available power that can be processed at each step of the emulation. This power corresponds to what an ideal 5 kW inverter would be capable of processing, assuming 100 % efficiency. As observed, inverter C exhibited the lowest performance ratio, limiting its delivered power due to the rise in temperature of its internal components.

Inverter B showed a more promising performance, yet still with limitations. According to the graph, this device did not reach the specified 5 kW, indicating that its thermal characteristics constrained its generation.

Finally, inverter A demonstrated the best behavior among all tested inverters. It was able to deliver its rated nominal power throughout almost the entire test. From 12:30 h onwards, as seen in the graph, it began to undergo thermal derating; however, it continued to deliver its nominal power until the end of the test. Based on the obtained and post-processed results, and by applying Equation 1, it was possible to calculate the performance ratio achieved by each device. Table 2 summarizes the results obtained.

Table 2: Comparison Results between inverters.

Description	Inverter A	Inverter B	Inverter C
Operating condition			
%DCor	1.36	1.36	1.36
%VDCnom	0.77	0.84	0.77
%IDCmax	0.99	0.82	0.95
Experimental results			
Peak output power (W)	5020.00	4888.00	4662.00
Einv (kWh)	40.74	40.15	37.80
Eideal,inv (kWh)	41.69	41.69	41.69
PRinv (%)	97.7%	96.3%	90.7%

As shown in the figure, it is possible to determine an index that quantitatively evaluates each device by employing the same testing methodology for all of them. As observed, Inverter C exhibited the lowest performance, with a PR of 90.7%. Inverter B, on the other hand, presented a PR of 96.3%. Finally, Inverter A achieved a PR of 97.7%. The thermal analysis comparison can be observed in Figure 6.

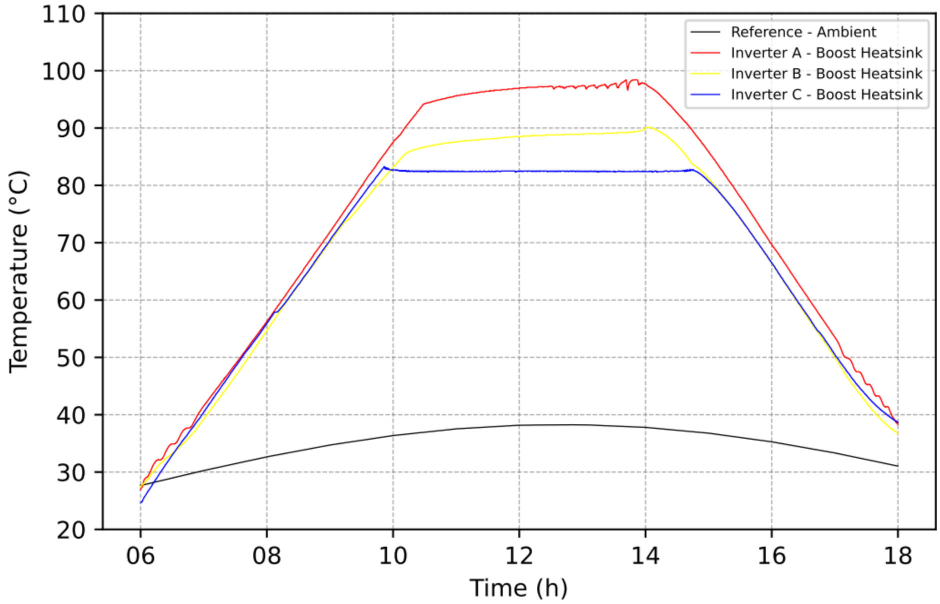

Figure 6: Comparison between 3 inverters boost heatsink temperature considering same test procedure.

As shown in Figure 6, the thermal comparison among the three inverters can be observed. Inverter A exhibits the highest thermal gradient, reaching temperatures above 95°C. Inverter B, represented in yellow, shows intermediate thermal values, with a peak temperature close to 90°C. Finally, Inverter C displays the lowest thermal values, limiting its temperature to approximately 83°C. Table 3 summarizes thermal analysis results.

Table 3: Comparison Results between inverters – thermal comparison.

Description	Inverter A	Inverter B	Inverter C
Maximum internal temperature measurements			
Bus Capacitor	85.6 ºC	78.5 ºC	89.0 ºC
Internal Air	75.8 ºC	73.5 ºC	71.6 ºC
Boost PCB	105.4 ºC	86.0 ºC	74.1 ºC
Inverter PCB	95.3 ºC	86.3 ºC	82.8 ºC
Boost Switch	99.3 ºC	84.8 ºC	84.0 ºC
Maximum external temperature measurements			
Boost heatsink	95.8 ºC	78.3 ºC	86.4 ºC
Inverter heatsink	102.4 ºC	90.1 ºC	83.3 ºC
Ambient	39.1 ºC	39.0 ºC	39.4 ºC
Front Cover	59.3 ºC	57.4 ºC	58.3 ºC

Table 3 shows that the largest thermal gradients are present in the equipment that achieved the highest performance ratio. This demonstrates that the performance ratio is closely linked to the thermal dynamics of the IUT, and a thermal analysis should always be considered when discussing energy conversion efficiency. The proposed methodology seeks to present quantitative and realistic results through tests on typical days, with thermal control and emulation of daily profiles.

4. Conclusions and future works

According to the results obtained, the efficiency of photovoltaic inverters is strongly influenced by their operating temperature. To address this, a novel methodology based on a redefined performance ratio was proposed. This approach enables the emulation of inverter operation under controlled thermal conditions, allowing the estimation of the actual energy generation expected in real-world scenarios, given specific irradiance and temperature profiles.

Through the proposed procedure, it was possible to quantitatively determine the performance index of each inverter, providing a fair and consistent basis for comparison among different models. The methodology enhances the accuracy of energy yield estimations by incorporating thermal effects that can be reproduced within the developed climatic chamber.

Consequently, this framework enables comparative assessment of multiple devices under representative environmental conditions from different regions of the country. Future work will focus on investigating the long-term influence of temperature on inverter reliability, aiming to establish a correlation between operating temperature and component lifetime degradation.

5. Acknowledgments

This study was financed in part by the Coordenação de Aperfeiçoamento de Pessoal de Nível Superior – Brazil (CAPES/PROEX) – Finance Code 001.

The authors would like to express their gratitude to Huawei for kindly providing the inverters used during the experimental tests.

6. References

Agência Nacional de Energia Elétrica (ANEEL), 2023. Resolução Normativa nº 1.059, de 24 de outubro de 2023: Aprimora as regras aplicáveis à microgeração e minigeração distribuída. Available at: https://www.aneel.gov.br (accessed July 2025).

Associação Brasileira de Energia Solar Fotovoltaica (ABSOLAR), 2025. Dados atualizados do setor solar fotovoltaico brasileiro. Available at: https://www.absolar.org.br (accessed July 2025).

Empresa de Pesquisa Energética (EPE), 2023. Plano Decenal de Expansão de Energia 2033. Brasília: EPE. Available at: https://www.epe.gov.br/pt/publicacoes-dados-abertos/publicacoes (accessed July 2025).

European Committee for Electrotechnical Standardization (CENELEC), 2010. EN 50530: Overall efficiency of grid-connected photovoltaic inverters. Brussels: CENELEC.

International Electrotechnical Commission (IEC), 2022. IEC 62891: Photovoltaic (PV) inverters – Procedures for temperature and power derating tests. Geneva: IEC.

Ineichen, P., 2008. A broadband simplified version of the Solis clear sky model. Solar Energy 82 (8), 758–762.

Kratochvil, J.A., Boyson, W.E., King, D.L., 2004. Photovoltaic array performance model. Available at: https://www.osti.gov/biblio/919131 (accessed July 2025).

Lima, G.P. de, et al., 2023. Comparing temperature derating test in the laboratory with commercial photovoltaic inverter datasheet. In: 2023 IEEE 8th Southern Power Electronics Conference and 17th Brazilian Power Electronics Conference (SPEC/COBEP), pp. 1–7.

Parton, W.J., Logan, J.A., 1981. A model for diurnal variation in soil and air temperature. Agricultural Meteorology 23, 205–216.

Perez, R., et al., 1987. A new simplified version of the Perez diffuse irradiance model for tilted surfaces. Solar Energy 39 (3), 221–232.

Soto, W.D., Klein, S.A., Beckman, W.A., 2006. Improvement and validation of a model for photovoltaic array performance. Solar Energy 80 (1), 78–88.